Seismic Demand Uncertainty provided by Ground Motion Intensity Measure

C. Cantagallo, G. Camata & E. Spacone
University "G. D'Annunzio" of Chieti-Pescara, Italy

R. Corotis
University of Colorado at Boulder, USA

SUMMARY:
The seismic demand generated by Nonlinear Dynamic Analyses is obtained by using ground motion records having different intensities. The uncertainty and the variability of the seismic demand are highly dependent on the variable adopted as intensity measure (IM). This generates the need to evaluate the dispersion of the demand measure in relation to different IMs. For this purpose, correlations between the maximum inter-story drift demand of nine reinforced concrete structures and a number of widely used ground motion intensity parameters are investigated. To determine the optimum parameter to be used as IM, two additional intensity parameters are analyzed, the spectral acceleration corresponding to the cracked and non-linear period of each structure, $S_a(T_{crack})$ and $S_a(T^*)$, respectively. The results show that these two intensity measures have the best correlation with the deformation demand and their use produces a lower variability of the seismic demand.

Keywords: Ground Motion, Intensity Measure, Reinforced concrete, Nonlinear dynamic analysis

1. INTRODUCTION

The evaluation of the seismic demand variability is fundamental in earthquake engineering as a higher uncertainty increases the capacity that must be designed into the system. This paper shows that the variability of the seismic demand related to the application of different records can vary significantly depending both on the chosen ground motion intensity measure and on the type of structure in relation to its level of non-linearity.

After selecting two different sets of un-scaled ground motions, one for the Ultimate Limit State (ULS) and one for the Damage Limit State (DLS), ground motion intensity parameters (GMI's) are calculated for each ground motion record. Nine different reinforced concrete structures are subjected to the selected records and analyzed using nonlinear dynamic analyses. Finally, for each structure, the ground motion intensity measures are related with the corresponding deformation demands and the dispersion of the demand measure in relation to each IM is evaluated through correlation coefficients.

Since the variability of deformation demand varies significantly in relation to the considered IM, various GMI's are analyzed, considering both those derived directly from the ground motions and those derived from the response spectra. To find GMI's having a good correlation with the structural demand also when ground motion records produce a nonlinear behaviour, two additional intensity parameters are considered: the spectral acceleration corresponding to the cracked period $S_a(T_{crack})$ and the spectral acceleration corresponding to the nonlinear period $S_a(T^*)$ of each structure.

2. SELECTION AND PROCESSING OF GROUND MOTION RECORDS

The record selection used in this study is based on Probabilistic Seismic Hazard Analysis (PSHA) derived from an Italian study carried out between 2004 and 2006 by the National Institute of Geophysics and Volcanology (INGV) and the Department of Civil Protection (DPC). This work

provides the seismic hazard analysis and the disaggregation for each point of a regular grid made of approximately 16852 nodes analyzing the entire Italian territory [*http://ess1.mi.ingv.it/*].

Ground motion records are selected using an earthquake scenario with moment magnitude M_w, epicentral distance R and soil site class A. The M_w-R bins are derived from seismic hazard disaggregation (Bazzurro and Cornell, 1999) which defines M_w and R providing the larger contribution to the seismic hazard at a specified probability of exceedance (Spallarossa and Barani, 2007).

For the analyses presented in this study, a site located on rock soil in Sulmona (AQ), 42.084° latitude and 13.962° longitude was selected. For the probability of exceedance of 50% in 50 years (Damage Limit State - DLS) 85 records with M_w between 5 and 6 and R between 15 and 30 km were selected, while for a probability of exceedance of 10% in 50 years (Ultimate Limit State - ULS) 61 records with M_w between 5.5 an 6.5 and R between 15 and 30 km were selected. Epicentral distances smaller than 15 km were not considered in order to avoid "near-field" effects. The M_w versus R plots for the two considered limit states are shown in Figure 2.1.

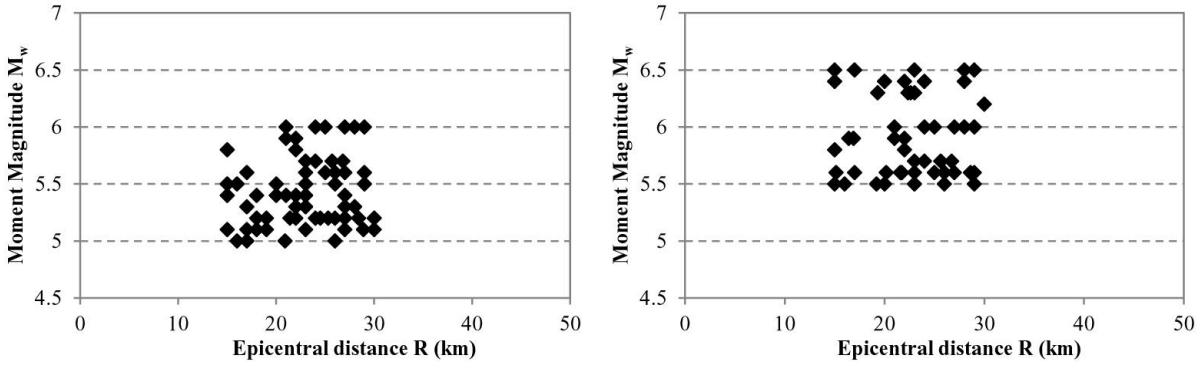

Figure 2.1. Magnitude versus epicentral distance plot for the records selected for the probabilities of exceedance of 50% in 50 years (at left) and 10% in 50 years (at right)

The selected records were subsequently taken from two databases: the European Strong-Motion Database (ESD) and the Italian Accelerometric Archive (ITACA). In these databases the components of ground motion (two horizontal and one vertical) are given with the orientation in which they were recorded. In general, these components are correlated because they are not oriented along the principal directions of the ground motion (Penzien and Watabe, 1975). Recorded accelerograms were then uncorrelated using a transformation of coordinates identical in form to those used in the transformation of stress (Lopez et al., 2004).

3. STRUCTURAL MODELS

The purpose of this study is to measure the variability of deformation demand with ground motion intensity. This objective requires an evaluation of a large number of structural models, whose principal geometrical and mechanical properties are briefly summarized in Table 3.1. and Figure 3.1.

Table 3.1. Principal geometrical and mechanical properties of the analyzed structures

Structure			Columns		Elastic Period T_1		
Structure (n.)	Height (m)	Plan Dimension (m)	Columns Section (cm)	Columns Bars (Φ)	Mode 1 (sec)	Mode 2 (sec)	Mode 3 (sec)
S 1	3	5 x 5	30x30 (C20/25)	4Φ12 (f_y=430 MPa)	0.17	0.17	0.16
S 2	3	15 x 5	30x60 (C20/25)	4Φ14 (f_y=430 MPa)	0.16	0.11	0.07
S 3	6	5 x 5	30x30 (C20/25)	4Φ12 (f_y=430 MPa)	0.41	0.41	0.37
S 4	6	15 x 5	30x60 (C20/25)	4Φ14 (f_y=430 MPa)	0.29	0.23	0.18
S 5	6	15 x 5	20x50 (C20/25)	4Φ10 (f_y=430 MPa)	0.44	0.30	0.23

S 6	6	15 x 5	20x40 (C20/25)	4Φ10 (f_y=215 MPa)	0.52	0.43	0.18
S 7	9	15 x 5	20x40 (C20/25)	4Φ10 (f_y=430 MPa)	0.92	0.86	0.27
S 8	9	15 x 10	20x40 (C20/25)	4Φ10 (f_y=430 MPa)	0.90	0.76	0.25
S 9	9	15 x 5	20x40 (C20/25)	4Φ10 (f_y=375 MPa)	0.67	0.61	0.45

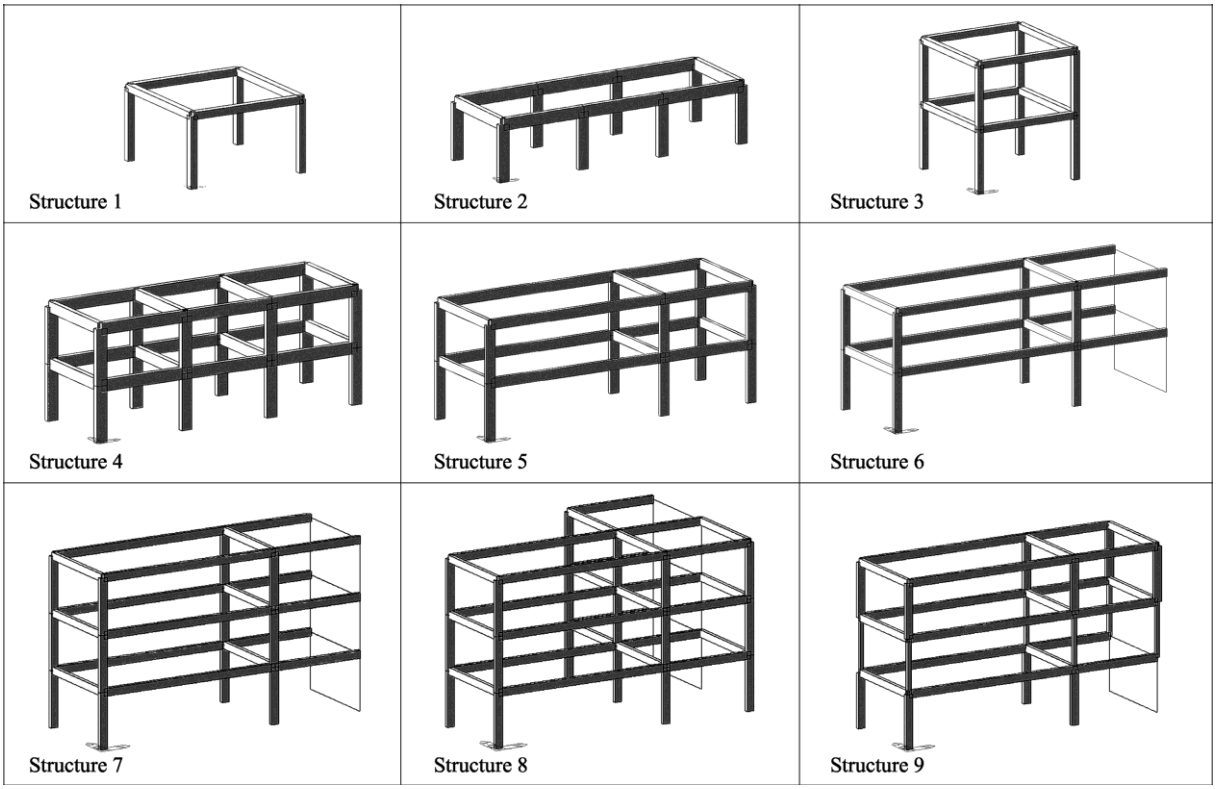

Figure 3.1. Reinforced concrete frame structures

Models were developed with the computer software Midas Gen 7.21 (Midas, 2007). The NonLinear Time History Analyses (NLTHA) were carried out using a force-based fiber beam model (Spacone et al., 1996). The concrete was modelled with the Kent and Park model (Kent and Park, 1971) with f_{ck} = 20 MPa, ε_{c0} = 0.003 and ε_{cu} = 0.0165. The steel nonlinear behaviour was described by the Menegotto-Pinto (Menegotto and Pinto, 1973) model with f_{yk} = 215, 375 or 430 MPa, E = 200 GPa and b = 0.02. In order to account for the real structural behaviour of frames, gravity loads were applied statically before the earthquake excitation was applied dynamically.

4. CORRELATION OF DEFORMATION DEMAND WITH GROUND MOTION INTENSITY

4.1. Ground motion intensity parameters

A large number of parameters are used to characterize the nature of the earthquake ground-motion. In general, they can be classified into two groups:

- parameters computed from the ground motion records
- parameters computed from the response spectra

Among the parameters that may be calculated from the ground motion records, those examined in this study are the Peak Ground Acceleration (PGA) and the Peak Ground Velocity (PGV). Parameters calculated from pseudo-acceleration response spectra are the spectral acceleration corresponding to the fundamental period of vibration of the structure $S_a(T_1)$, the Housner Intensity HI (Housner, 1952), corresponding to the area below the pseudo velocity spectrum in the period range 0.1-2.5 sec, and the Acceleration Spectrum Intensity ASI (Von Thun et al., 1988), corresponding to the area below the

pseudo acceleration spectrum in the period range 0.1-0.5 sec. In particular, it should be noted that $S_a(T_1)$ provides the response of a linear single-degree-of-freedom structure with a period of vibration approximately equal to the first-mode period of the MDOF structure under consideration, but the response of an MDOF structure is also affected by excitation of higher mode of the structure at period shorter than T_1. In addition, S_a at periods longer than T_1 may affect the structure behaviour because, as the structure starts behaving non-linearly, the effective period of its first mode increases to a period larger than T_1 (Baker and Cornell, 2005). For these reasons, two intensity parameters are further examined, the spectral acceleration corresponding to a "cracked period", $S_a(T_{\text{crack}})$ to take into account that the structure is already partially cracked after the application of gravity loads, and the spectral acceleration corresponding to a "non linear period", $S_a(T^*)$. The two periods T_{crack} and T^* are obtained from nonlinear static (pushover) analyses, according to the Eurocode 8 requirements. In particular after subjecting the structures to the gravity loads, two vertical distributions of lateral loads are applied to each structure, a "uniform" pattern, based on mass proportional lateral forces and a "modal" pattern, proportional to the first mode lateral force distribution in the direction under consideration. Capacity curves representing the relation between base shear force and control node displacement of the MDOF systems are subsequently transformed in capacity curves representing equivalent Single Degree of Freedom (SDOF) systems through the building of bilinear elasto-perfectly plastic force – displacement curves. The periods T_{crack} and T^* are obtained as the periods corresponding, respectively, to the first step of the SDOF equivalent curve and to the bilinear idealized curve. In particular it should be noted that while T_{crack} corresponds to the period obtained after the application of gravity loads, T^* is a term that represents the approximate nonlinear behaviour of the entire structure and can be calculated with the Eqn. 4.1, where d_y^* and F_y^* are the yield displacement and the ultimate strength of the bilinear idealized system, and m^* is the mass of the equivalent SDOF system (Eurocode 8, 2005: Annex B). Table 4.1 shows the T_{crack} and T^* values for each structure and considered load distribution.

$$T^* = 2\pi\sqrt{\frac{m^* d_y^*}{F_y^*}} \tag{4.1}$$

Table 4.1. T_{crack} and T^* values obtained from pushover analyses of the nine considered structures

Structure n.	Uniform Distribution		Modal Distribution	
	T_{crack} (sec)	T^* (sec)	T_{crack} (sec)	T^* (sec)
Structure 1	0.24	0.35	---	---
Structure 2	0.28	0.49	---	---
Structure 3	0.48	0.65	0.52	0.69
Structure 4	0.40	0.72	0.42	0.77
Structure 5	0.61	1.21	0.67	1.20
Structure 6	0.56	0.90	0.74	1.25
Structure 7	0.91	1.21	1.24	1.75
Structure 8	0.93	1.07	1.43	1.61
Structure 9	0.77	0.99	0.96	1.39

For each record it is possible to obtain three values of each seismic parameter, corresponding to each of three ground motion components. In this paper, the vertical component of motion was neglected and each structure was only subjected to the two orthogonal horizontal ground motion components. In order to correlate the GMI's to the Engineering Demand Parameter (EDP), it was necessary to represent the two components of each intensity parameter by a single parameter, corresponding to the geometric mean of the values obtained, respectively, in the *x* direction and *y* directions. The geometric mean is now the most widely used horizontal-component definition (Beyer and Bommer, 2006) and more specifically for the spectral acceleration S_a corresponding to a period T_i it is defined by Eqn. 4.2.

$$S_a\ T_i\ = \sqrt{S_{ax}\ T_i\ \cdot S_{ay}\ T_i\ } \tag{4.2}$$

As can be easily demonstrated, the geometric mean is equal to the anti-log of the lognormal average of

the two horizontal components.

4.2. Ground motion intensity parameters

Ground motion intensity parameters of selected records were analyzed selecting the probability distribution more consistent with the empirical distribution derived from the selected record intensity parameters. Figure 4.1 shows the empirical distributions of the ground motion intensity measures obtained from the 85 records selected at the DLS (the spectral accelerations correspond to the structural periods of Structure 1).

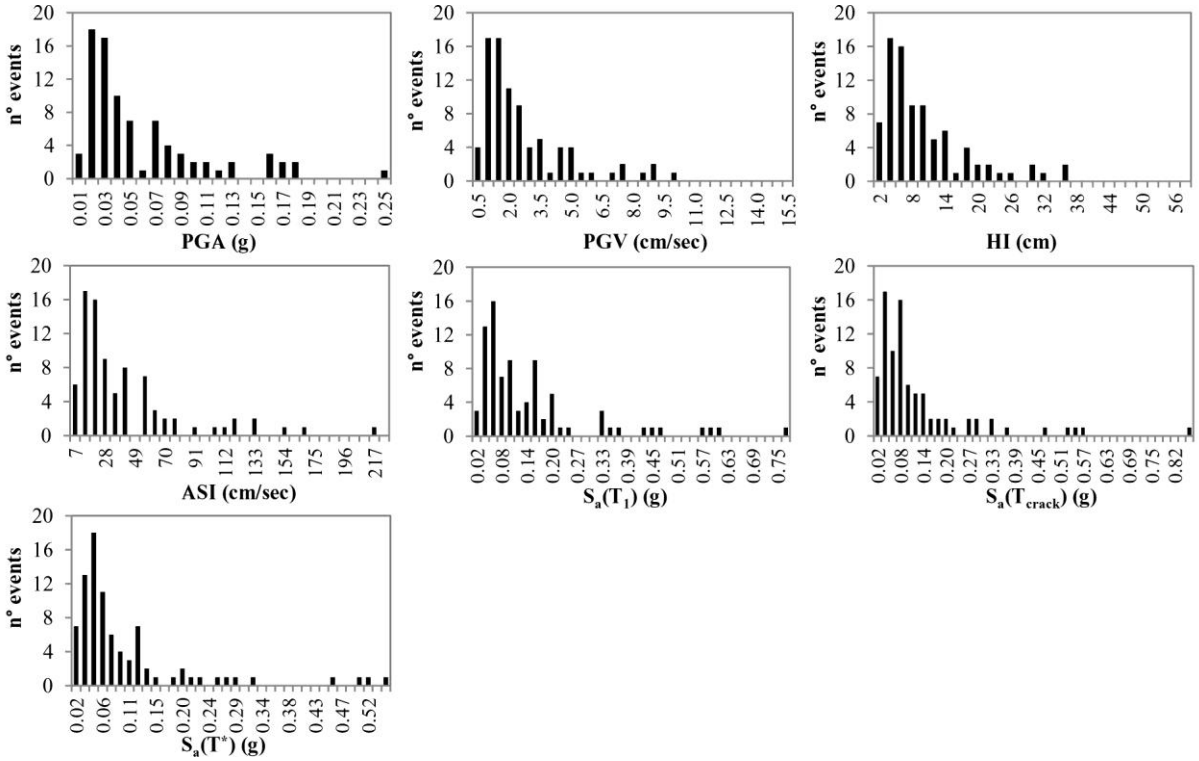

Figure 4.1. Empirical Probabilistic Distribution Functions (PDF) of the 7 GMI's analyzed for the record selected at the DLS (spectral acceleration parameters correspond to Structure 1)

In order to identify whether the input distributions were better represented by a normal or lognormal distribution, the Kolmogorov-Smirnov Test was adopted, as depicted in Figure 4.2. In statistics, the Kolmogorov–Smirnov test (K–S test) is a nonparametric test used to compare a sample with a reference probability distribution. For the selected ground motion set at the DLS, the Kolmogorov–Smirnov test indicates that the probability distribution that best approximates the intensity parameters is the lognormal, and this is true especially for low intensity values.

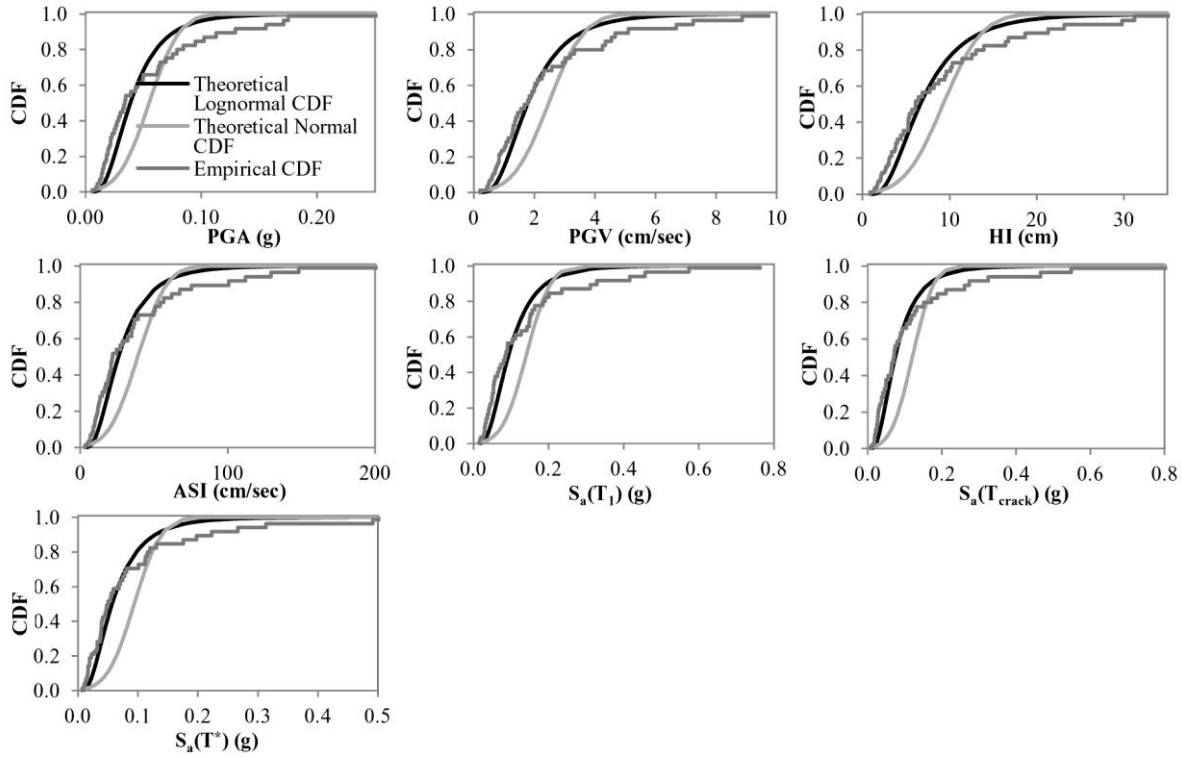

Figure 4.2. Empirical and theoretical Cumulative Distribution Functions (CDF) of the 7 GMI's analyzed for the record selected at the DLS (spectral acceleration parameters correspond to Structure 1)

4.3. The Engineering Demand Parameter

The EDP considered in this study is the Maximum Inter-story Drift Ratio (MIDR). For each pair of accelerograms applied along the direction 0°/90°, the displacements of the node corresponding to the center of mass in *x* (DX) and *y* directions (DY) of each floor were calculated. Then these displacements were combined according to Eqn. 4.3.

$$\mathrm{DXY} = \sqrt{\mathrm{DX}^2 + \mathrm{DY}^2} \tag{4.3}$$

4.4. Correlation between maximum inter-storey drift demand and ground motion intensity parameters

After calculating for each structure and for each recording the MIDR's DXY, these displacements have been correlated with the intensity parameters previously considered. The goodness of the correlations was evaluated through coefficients of determination R^2 whose values are calculated by using Eqn. 4.4, where Y_i = observed values, Y_m = mean of the observed data, Y_{pi} = data obtained from the regression model and n = total number of points:

$$R^2 = \frac{\sum_i^n \left(Y_{pi} - Y_m \right)^2}{\sum_i^n \left(Y_i - Y_m \right)^2} \tag{4.4}$$

The values of coefficients R^2 were based on linear and polynomial regression lines fitted through the data. The forms of linear and exponential relationships are $y = ax + c$ and $y = ax + bx^2$, where a, b and c are constant coefficients.

5. RESULTS

Figure 5.1 and Figure 5.2 show the relationships between the selected GMI's and MIDR's of Structure 1 respectively at the DLS and ULS. The R^2 values derived from the correlations between maximum inter-story drift demands of all the nine analyzed frames and GMI's selected at the DLS and ULS represented respectively in Table 5.1 and Table 5.2 suggest that in most cases $S_a(T_{\text{crack}})$ and $S_a(T^*)$ have stronger correlation with the output than other intensity parameters.

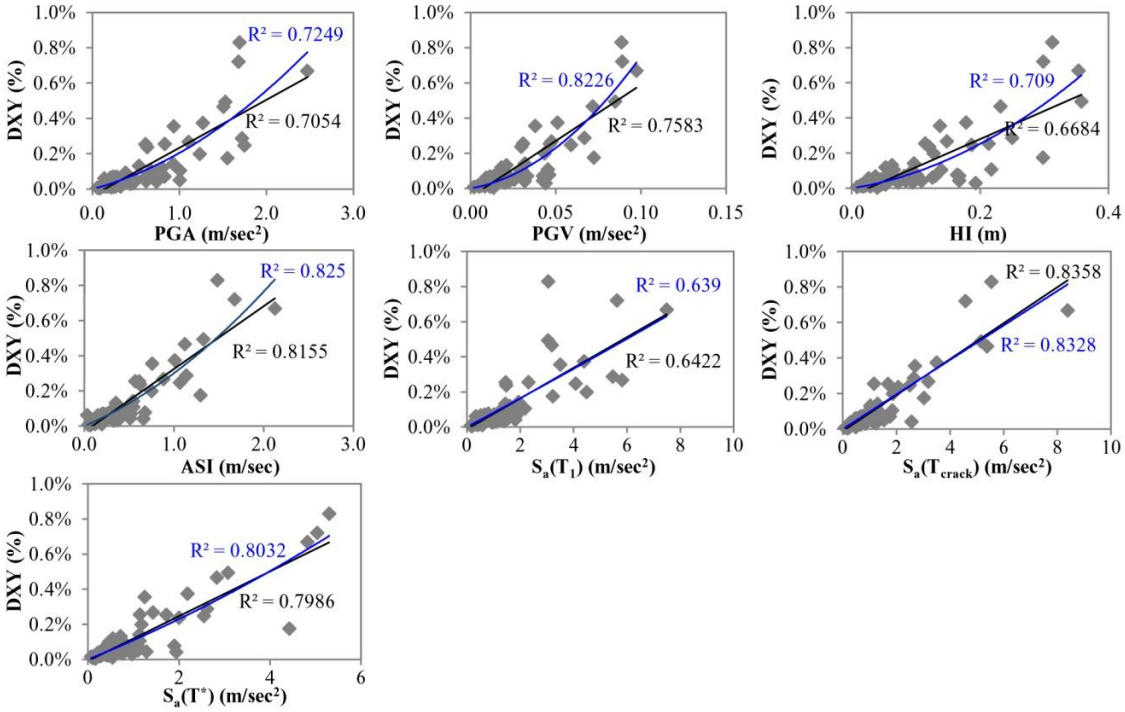

Figure 5.1. Correlations between the selected GMI's and MIDR's for Structure 1 at the DLS

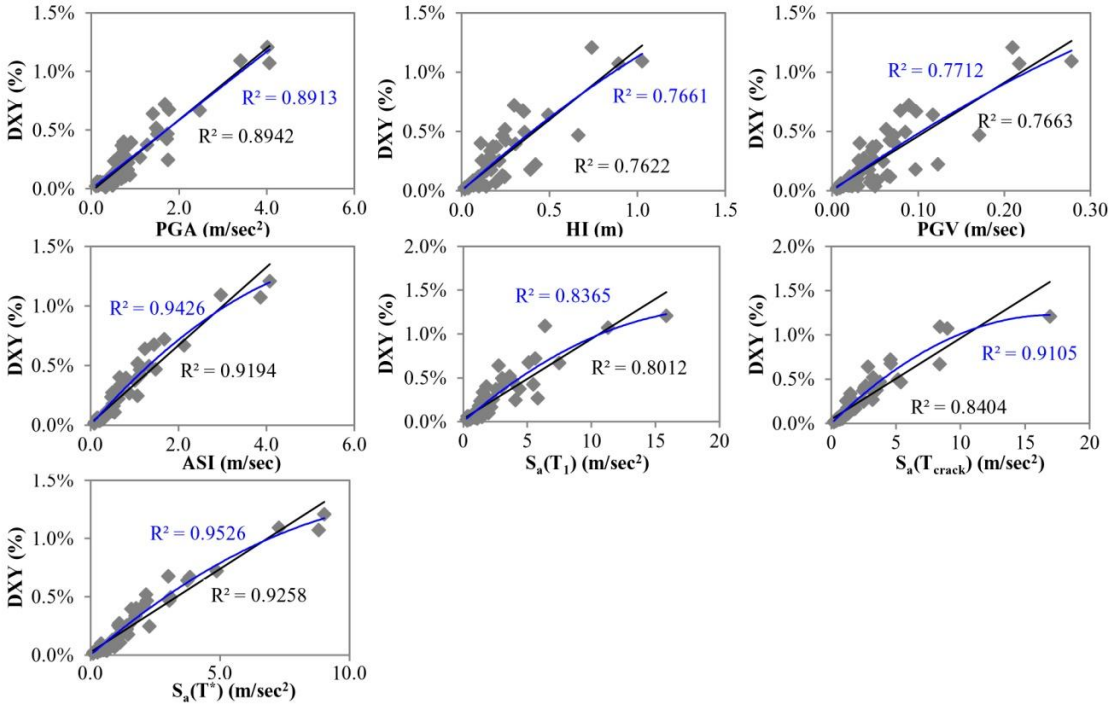

Figure 5.2. Correlations between the selected GMI's and MIDR's for Structure 1 at the ULS

Table 5.1. Correlation of Ground Motion Intensity Parameters (GMI) with Maximum Inter-story Drift Ratio (MIDR) at the Damage Limit State DLS

Coefficients of Determination (R^2)														
Str.	Linear ($y = ax + c$)							Nonlinear ($y = ax + bx^2$)						
n.	PGA	HI	PGV	ASI	$S_a(T_1)$	$S_a(T_{crack})$	$S_a(T^*)$	PGA	HI	PGV	ASI	$S_a(T_1)$	$S_a(T_{crack})$	$S_a(T^*)$
S 1	0.71	0.67	0.76	0.82	0.64	0.84	0.80	0.71	0.67	0.76	0.82	0.64	0.84	0.80
S 2	0.63	0.62	0.71	0.74	0.50	0.78	0.78	0.63	0.62	0.71	0.74	0.50	0.78	0.78
S 3	0.53	0.79	0.73	0.64	0.77	0.91	0.95	0.53	0.79	0.73	0.64	0.77	0.91	0.95
S 4	0.74	0.77	0.84	0.85	0.87	0.88	0.77	0.74	0.77	0.84	0.85	0.87	0.88	0.77
S 5	0.66	0.86	0.82	0.77	0.86	0.84	0.86	0.66	0.86	0.82	0.77	0.86	0.84	0.86
S 6	0.57	0.86	0.80	0.70	0.89	0.91	0.90	0.57	0.86	0.80	0.70	0.89	0.91	0.90
S 7	0.51	0.79	0.71	0.50	0.90	0.90	0.92	0.51	0.79	0.71	0.50	0.90	0.90	0.92
S 8	0.50	0.77	0.70	0.53	0.90	0.92	0.92	0.50	0.77	0.70	0.53	0.90	0.92	0.92
S 9	0.53	0.77	0.70	0.59	0.75	0.87	0.94	0.53	0.77	0.70	0.59	0.75	0.87	0.94

Table 5.2. Correlation of Ground Motion Intensity Parameters (GMI) with Maximum Inter-story Drift Ratio (MIDR) at the Ultimate Limit State ULS

Coefficients of Determination (R^2)														
Str.	Linear ($y = ax + c$)							Nonlinear ($y = ax + bx^2$)						
n.	PGA	HI	PGV	ASI	$S_a(T_1)$	$S_a(T_{crack})$	$S_a(T^*)$	PGA	HI	PGV	ASI	$S_a(T_1)$	$S_a(T_{crack})$	$S_a(T^*)$
S 1	0.89	0.76	0.77	0.92	0.80	0.84	0.93	0.89	0.77	0.77	0.94	0.84	0.91	0.95
S 2	0.85	0.64	0.66	0.87	0.79	0.87	0.71	0.85	0.64	0.66	0.87	0.79	0.88	0.73
S 3	0.66	0.83	0.83	0.67	0.82	0.89	0.94	0.66	0.86	0.86	0.68	0.82	0.89	0.95
S 4	0.86	0.86	0.86	0.87	0.89	0.93	0.77	0.86	0.87	0.86	0.87	0.90	0.93	0.79
S 5	0.69	0.91	0.88	0.69	0.86	0.87	0.79	0.69	0.92	0.89	0.71	0.86	0.89	0.80
S 6	0.72	0.90	0.90	0.73	0.94	0.95	0.87	0.72	0.91	0.90	0.74	0.93	0.95	0.87
S 7	0.57	0.89	0.87	0.55	0.91	0.91	0.90	0.58	0.89	0.87	0.58	0.91	0.91	0.90
S 8	0.58	0.88	0.86	0.55	0.90	0.92	0.94	0.58	0.88	0.86	0.59	0.91	0.92	0.94
S 9	0.54	0.85	0.83	0.50	0.78	0.81	0.94	0.54	0.85	0.83	0.55	0.79	0.82	0.94

Since only some records generate a nonlinear behavior of the structures, a heteroscedastic model was developed. In statistics, a sequence of random variables is heteroscedastic if the random variables have different variances and can be described by different distributions for different values of the independent variables. Also MIDR's can be described by different distributions depending on the structure behavior, linear or nonlinear. In particular when ground motion records provided a nonlinear structural demand, MIDR's were related with $S_a(T^*)$ and correlations were found through polynomial regression lines, while for linear demands, MIDR's were related with $S_a(T_{crack})$, and data were fitted through linear relationships.

Heteroscedastic models for the nine structures analyzed subjected to the 61 records selected for the ULS are shown in Figure 5.3, while correlation coefficients for the DLS and the ULS are summarized in Table 5.3. Heteroscedastic models show that the spectral accelerations corresponding to the periods T_{crack} and T^* provide, in most cases, good correlations with maximum inter-story drift ratios, in both cases for linear and nonlinear structural demand.

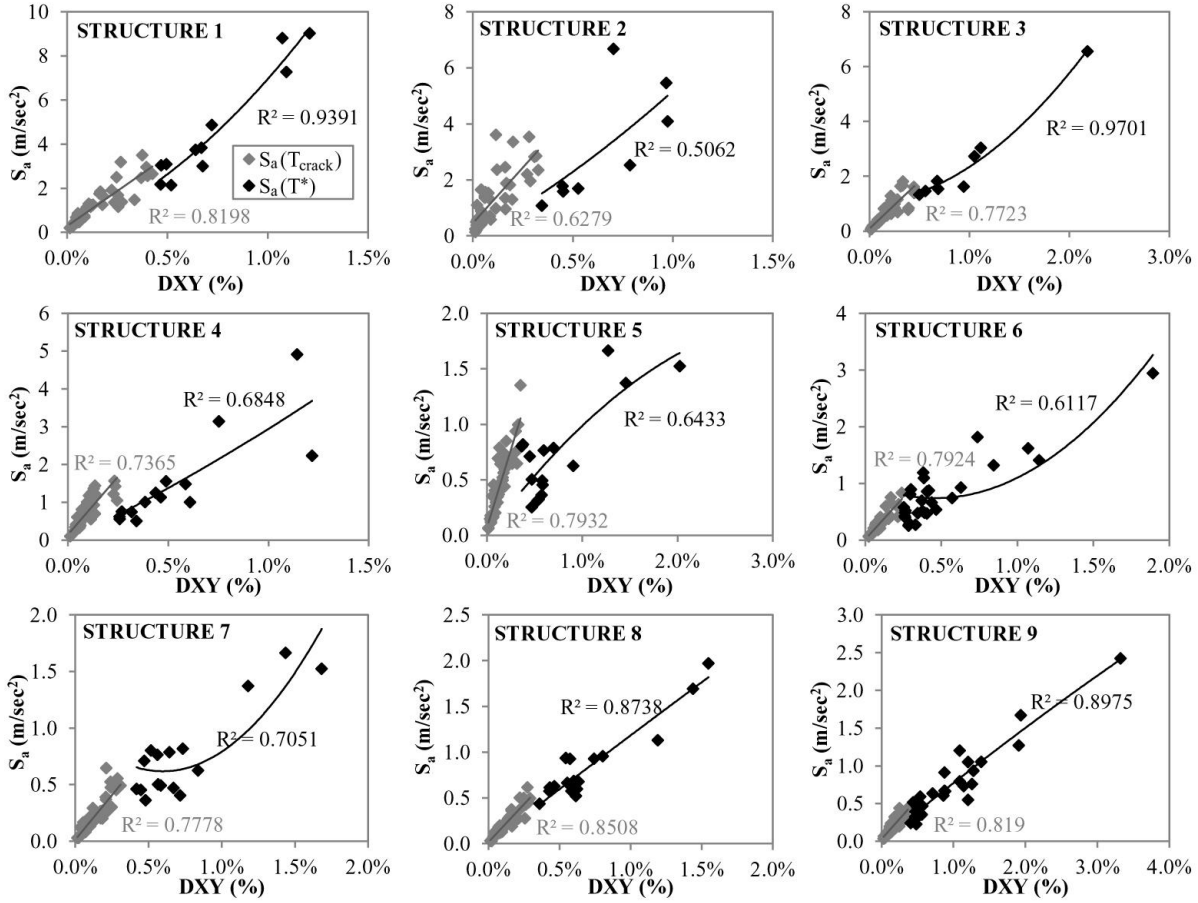

Figure 5.3. Mathematical models for non-linear response history analysis

Table 5.3. Correlation Coefficients of heteroscedastic models for the nine structures analyzed subjected respectively to the 85 records selected for the ULS and the 61 records selected for the ULS.

Coefficients of Determination (R^2)				
Structure n.	Damage Limit State (DLS)		Ultimate Limit State (ULS)	
	Linear demand ($y = ax + c$) on $S_a(T_{crack})$	Nonlinear demand ($y = ax + bx^2$) on $S_a(T^*)$	Linear demand ($y = ax + c$) on $S_a(T_{crack})$	Nonlinear demand ($y = ax + bx^2$) on $S_a(T^*)$
Structure 1	0.7102	0.9357	0.8198	0.9391
Structure 2	0.6666	0.7486	0.6279	0.5062
Structure 3	0.8817	0.7755	0.7723	0.9701
Structure 4	0.7511	0.4367	0.7365	0.6848
Structure 5	0.8671	0.5780	0.7932	0.6433
Structure 6	0.8430	0.6601	0.7924	0.6117
Structure 7	0.7732	0.6037	0.7778	0.7051
Structure 8	0.8685	0.7047	0.8508	0.8738
Structure 9	0.8336	0.8010	0.8190	0.8975

6. DISCUSSION AND CONCLUSIONS

In this article a method for the estimation of the correlation between GMI's and MIDR's was presented. Nine tridimensional frames under a suite of 85 pairs of records selected for the DLS and 61 pairs of records selected for the ULS were analyzed through non-linear time history analysis. The degree of correlation was expressed by determination coefficients through homoscedastic and heteroscedastic models, depending on whether the entire set of records was considered or if the records were divided as a function of the structural response obtained, linear or nonlinear. In

agreement with the published literature (Yakut and Yilmaz, 2008) this work shows that PGA provides a poor correlation with the MIDR whereas spectral and energy parameters provide in general a good correlation.

Two non conventional intensity parameters were also used, $S_a(T_{crack})$ and $S_a(T^*)$. T_{crack} and T^* were obtained from a nonlinear static (pushover) analysis and represent the period of the cracked structure after the application of gravity loads and the period of the nonlinear structure, respectively. These two spectral acceleration parameters provide in most cases a better correlation with the selected EDP, and these results indicate that uncertainties associated with deformation demands produced by earthquakes of different intensities can be reduced by using these IMs. Finally, since the parameter $S_a(T^*)$ may be difficult to calculate in practice, in particular for complicated structures, in order to reduce the variability of the response generated from earthquakes of various intensities, the authors suggest using $S_a(T_{crack})$ as intensity measure.

AKCNOWLEDGEMENT

The authors would like to acknowledge the financial support from the ReLUIS program of the Italian Civil Protection Agency (DPC), task 1.1.2, contract n. 823, 24/09/2009.

REFERENCES

Bazzurro, P. and Cornell, C.A. (1999). Disaggregation of seismic hazard. *Bulletin of the Seismological Society of America* **89:2**, 501-520.

Spallarossa, D. and Barani, S. (2007). Progetto DPC-INGV S1, Deliverable D14. *http://esse1.mi.ingv.it/d14.html*

Penzien, J. and Watabe, M. (1975). Characteristics of 3-dimensional earthquake ground motion. *Earthquake Engineering & Structural Dynamics* **3:4**, 365-374.

López, O.A., Bonilla, R., Hernández, J.J. and Fernández, A. (2004). Propiedades de las tres componentes principales del movimiento sísmico, *Boletín Técnico IMME* **42:1**, 1-28.

Spacone, E., Filippou, F.C. and Taucer, F. (1996). Fiber Beam-Column Model for Nonlinear Analysis of R/C Frames: I. Formulation. *Earthquake Engineering & Structural Dynamics* **25:7**, 711-725.

Kent, D.C. and Park, R. (1971). Flexural members with confined concrete. *Journal of the Structural Division* **97:7**, 1969–1990.

Menegotto, M. and Pinto, P.E. (1973). Method of analysis for cyclically loaded reinforced concrete plane frames including changes in geometry and nonelastic behavior of elements under combined normal force and bending. *IABSE Symposium on Resistance and Ultimate Deformability of Structures Acted on by Well-Defined Repeated Loads*, *Zurich*, 112–123.

Housner, G.W. (1952). Spectrum Intensity of strong-motion earthquake. *Proceeding of the Symposiucm on Earthquake and Blast effects on Structures*, EERI, Univ. of California at Los Angeles, Earthquake Engineering Research Institute, Oakland, 20-36.

Von Thun, J.L., Roehm, L.H., Scott, G.A. and Wilson, J.A. (1988). Earthquake ground motions for design analysis of dam. In: *Earthquake Engineering and Soil Dynamics II – Recent Advance in Ground-Motion Evaluation*. Geotechnical Special Publication **20**, ASCE, New York, 463-481.

Baker, J.W. and Cornell, C.A. (2005). A vector-valued ground motion intensity measure consisting of spectral acceleration and epsilon, *Earthquake Engineering & Structural Dynamics* **34:10**, 1193–1217.

Eurocode 8 (UNI EN 1998-1:2005). Design of structures for earthquake resistance.

Beyer, K. and Bommer J.J. (2006). Relationships between Median Values and between Aleatory Variabilities for Different Definitions of the Horizontal Component of Motion. *Bulletin of the Seismological Society of America* **96:4A**, 1512 – 1522.

Yakut, Y. and Yılmaz, H. (2008). Correlation of Deformation Demands with Ground Motion Intensity. *Journal of Structural Engineering* **134:12**, 1818-1828.